Available online at www.sciencedirect.com

ScienceDirect

IFAC PapersOnLine 52-12 (2019) 97–102

An Event-Triggered Predictive Controller for Spacecraft Rendezvous Hovering Phases

Julio C. Sanchez * **Christophe Louembet** **
Francisco Gavilan * **Rafael Vazquez** *

* *Departamento de Ingeniería Aeroespacial, Universidad de Sevilla, Sevilla, Spain (e-mails: jsanchezm@us.es, fgavilan@us.es, rvazquez1@us.es).*

** *LAAS-CNRS, Université de Toulouse, CNRS, Toulouse, France (e-mail: louembet@laas.fr).*

Abstract: This work presents an event-triggered model predictive controller for spacecraft hovering phases. The target is assumed to be inert on its an elliptic orbit whereas the chaser has impulsive thrusters. The main goal is to design a local controller based on event-triggering principle to maintain the spacecraft inside a given hovering region while minimizing fuel consumption and avoiding unnecessary small amplitude firings. Using hybrid impulsive systems theory and reachability analysis, the invariance of the proposed method is studied. Simulation results are shown and discussed.

Keywords: Event-triggered control, Predictive control, Impulsive control, Spacecraft rendezvous

1. INTRODUCTION

In the context of spacecraft rendezvous, the hovering phase consists of a chaser spacecraft maintaining its relative position within a bounded region with respect to a target spacecraft. This mission phase is especially relevant for orbit servicing operations with potential application to geostationary satellites servicing, see Barnhart et al. (2013), and spacecraft refuelling, see B. Reed et al. (2016).

In this paper, the target spacecraft is assumed to be passive and the chaser one is controlled by means of chemical thrusters so that the actuation can be modelled by an impulsive signal. Some relevant works on impulsive control for rendezvous operations include Breger and How (2008), Di Cairano et al. (2012) and Yang and Cao (2015) whereas formation flying is addressed by Qi et al. (2012) and Gaias and D'Amico (2015).

The purpose of this study is to design an event-triggered predictive control strategy to maintain the spacecraft within the limits of a defined polytopic zone. Arantes Gilz et al. (2017) achieved station-keeping by controlling the spacecraft motion in the set of periodic trajectories included in the zone of interest. However, since the impulse sequence is computed at a fixed period, the obtained controls can be unnecessary or too small to be executed by the thrusters, especially if the system belongs or is close to the admissible set.

To overcome these drawbacks, an event-triggered model predictive controller is considered in this work for station-keeping. Event-based control is a control methodology where the commands are asynchronously computed, reducing the communication needs between the sensors, the on-board computer and the actuators in the control loop (see Aström (2008) for the basics). This methodology can be combined with feedback policies, see Wu et al. (2014) and references therein, and model-predictive schemes, see Pawlowski et al. (2015). In the context of spacecraft operations, event based controllers are recently attracting the attention of the attitude control community, see Wu et al. (2018) and Zhang et al. (2018), whereas some initial work for rendezvous hovering phases can be found in Louembet and Arantes Gilz (2018).

The main contribution of this paper is the development of a predictive controller using impulsive control in an asynchronous way. Its control objective is to locally stabilize the set of relative trajectories included in a given polytopic subset space. The scientific challenges arise from the linear time-varying dynamics and from the limited capability of the spacecraft thrusters which can only produce thrust of a minimum and maximum magnitude.

The present work extends and completes the initial communication by Louembet and Arantes Gilz (2018) in several directions. The definitions of the control laws are refined and explicitly detailed. The trigger laws have been redefined to ensure that all possible cases are covered. Additionally, the invariance of the proposed control approach is studied by using hybrid impulsive systems theory (Haddad et al. (2006)).

⋆ The authors gratefully acknowledge financial support from Universidad de Sevilla through its V-PPI US and of the Spanish Ministerio de Ciencia, Innovación y Universidades under grant PGC2018-100680-B-C21.

10.1016/j.ifacol.2019.11.076

Note that the hybrid systems framework has been recently employed for orbital rendezvous applications. For instance, the recent invited session "A Spacecraft Benchmark Problem for Analysis & Control of Hybrid Systems" that was presented at the 2016 IEEE Conference on Decision and Control focused on this topic. Moreover, Brentari et al. (2018) studies the stability of relative orbits. The present paper focuses on the invariance of the set of periodic relative orbits that hover inside a given polytopic subspace. The proposed controller ensures local contractiveness.

The structure of this paper is as follows. Section 2 describes the relative motion model and the set of admissible orbits. Next, Section 3 presents both the control law and the trigger law. Section 4 studies the invariance of the proposed controller. Section 5 shows results for cases of interest. Finally, Section 6 closes this paper with some additional considerations.

2. PROBLEM STATEMENT

In this section, firstly the relative motion model used to design the control law is explained. Then, the set of the constrained relative orbits for the hovering phase is presented, and a formal description based on envelope functions is provided.

2.1 Modelling the relative motion

The relative motion of the chaser spacecraft, denoted by S_f, is expressed with respect to the local frame attached to a passive target spacecraft whose position is denoted by S_l. The local frame $\{S_l, \boldsymbol{x}, \boldsymbol{y}, \boldsymbol{z}\}$, denoted Local Vertical/Local Horizontal (LVLH), moves around the inertial Earth-centered frame, $\{O, \boldsymbol{I}, \boldsymbol{J}, \boldsymbol{K}\}$, along the target spacecraft orbit. Note that $\boldsymbol{z}$ is the radial position (positive towards the centre of the Earth), $\boldsymbol{y}$ is the cross-track position (opposite to the orbit angular momentum) and $\boldsymbol{x}$ is the in-track position completing a right-handed system.

Under Keplerian assumptions, the relative motion between two spacecraft can be expressed by means of the Tschauner-Hempel equations, see Tschauner (1967). Considering that $\|\overrightarrow{OS_l}\| \gg \|\overrightarrow{S_l S_f}\|$, these equations can be linearized to obtain the following linear time-varying dynamics

$$\dot{X}(t) = A(t)X(t), \tag{1}$$

where the state vector X represents the relative position and velocity in the LVLH frame

$$X(t) = [x(t),\, y(t),\, z(t),\, \dot{x}(t),\, \dot{y}(t),\, \dot{z}(t)]^T.$$

In this work, the transition matrix Φ of the dynamics (1) is exploited. Accordingly to Yamanaka and Ankersen (2002), after the change of the time variable to the true anomaly ν,

$$\tilde{X}(\nu) = T(\nu)X(t), \tag{2}$$

the transition matrix Φ is obtained such that

$$\tilde{X}(\nu) = \Phi(\nu, \nu_0)\tilde{X}(\nu_0), \quad \nu_0 \leq \nu. \tag{3}$$

In particular, the relative position can be explicitly expressed in a convenient manner as

$$\begin{aligned} \tilde{x}(\nu) &= d_1(1+\rho)s_\nu - d_2(1+\rho)c_\nu + d_3 + 3d_0 J(\nu)\rho^2, \\ \tilde{y}(\nu) &= d_4 c_\nu + d_5 s_\nu, \\ \tilde{z}(\nu) &= d_1\rho c_\nu + d_2\rho s_\nu - 3ed_0 J(\nu)s_\nu\rho + 2d_0, \end{aligned} \tag{4}$$

where $c_\nu = \cos(\nu)$, $s_\nu = \sin(\nu)$, $\rho = (1 + ec_\nu)$, e is the eccentricity of the target orbit and $J(\nu)$ is given by

$$J(\nu) := \int_{\nu_0}^{\nu} \frac{d\tau}{\rho(\tau)^2} = \sqrt{\frac{\mu}{a^3}}\frac{t - t_0}{(1-e^2)^{3/2}}. \tag{5}$$

As the orbital elements of a Keplerian orbit, the parameters d_0 to d_5 are integration constants that define the shape and position of the relative orbits, see (Deaconu, 2013, chap. 2). This fact makes the vector $D = [d_0,\, d_1,\, d_2,\, d_3,\, d_4,\, d_5]^T$ the relevant state when aiming to constrain relative orbits. Note that a linear transformation exists between the relative state $\tilde{X}$ and the vector D,

$$\tilde{X}(\nu) = F(\nu)D(\nu). \tag{6}$$

Since $\det F = 1 - e^2 \neq 0,\ \forall e \in [0, 1)$, it represents a similarity transformation and D is a proper state vector with its own dynamics $D'(\nu) = A_D(\nu)D(\nu)$ and its own transition matrix such that $D(\nu) = \Phi_D(\nu, \nu_0)D(\nu_0)$. The details are presented in (Deaconu, 2013, chap 2). Typically, for space hovering operations, the chaser spacecraft is controlled by chemical engines operating at high levels of thrust during short periods of time with respect to the target orbit period. In practice, this fact leads to instantaneous changes of velocities that can be modelled as impulses

$$X^+(t) = X(t) + B\Delta V(t), \text{ with } B = [0_3, \mathbb{I}_3]^T, \tag{7}$$

where 0_3 is the square null matrix and $\mathbb{I}_3$ is the identity matrix, both of dimension 3. Applying the changes of variables (2) and (6), an impulse at instant ν produces a jump in the state from D to D^+ as

$$D^+(\nu) = D(\nu) + B_D(\nu)\Delta V(\nu), \tag{8}$$

with

$$B_D(\nu) = F^{-1}(\nu)T(\nu)B, \tag{9}$$

and hence

$$B_D(\nu) = \frac{1}{k^2(e^2-1)\rho}\begin{bmatrix} \rho^2 & 0 & -es_\nu\rho \\ -2c_\nu - e(1+c_\nu^2) & 0 & s_\nu\rho \\ -s_\nu(2+ec_\nu) & 0 & 2e - c_\nu\rho \\ es_\nu(2+ec_\nu) & 0 & ec_\nu\rho - 2 \\ 0 & -(e^2-1)s_\nu & 0 \\ 0 & (e^2-1)c_\nu & 0 \end{bmatrix}.$$

Equation (8) shows that the influence of a given impulsive control, ΔV, depends on the application instant due to the time dependence of the input matrix B_D. Additionally, the thrust magnitude along each axis has to comply with the following conditions on deadzone and saturation

$$\underline{\Delta V} \leq |\Delta V| \leq \overline{\Delta V}. \tag{10}$$

2.2 Semi-algebraic description of the constrained orbits set

The goal of our predictive controller is to maintain the spacecraft hovering in a predefined polytopic subset of the relative position space. Thereafter, a cuboid is considered without loss of generality:

$$\underline{x} \leq x(t) \leq \overline{x},\ \underline{y} \leq y(t) \leq \overline{y},\ \underline{z} \leq z(t) \leq \overline{z}\,,\ \forall t \geq t_0. \tag{11}$$

The most economic way to hover in a given zone is that the chaser evolves on periodic orbits due to the absence of natural drift. In Deaconu (2012), the necessary and sufficient periodicity condition, namely $d_0 = 0$, has been established. Inserting the changes of variables (2) and (6)

into (11) and considering the periodicity condition, the admissible set S_D^p can be formally defined as

$$S_D^p := \left\{ D \in \mathbb{R}^6 \;\middle|\; d_0 = 0,\ \begin{array}{c} \underline{x} \le F_x(\nu) D \le \overline{x} \\ \underline{y} \le F_y(\nu) D \le \overline{y} \\ \underline{z} \le F_z(\nu) D \le \overline{z} \end{array},\ \forall \nu \right\}, \quad (12)$$

where F_x, F_y and F_z are, respectively the first three rows of F divided by ρ. The set S_D^p is described by linear but time-varying conditions on the state D.

In (Arantes Gilz et al., 2017, Section 3), an implicitization method is developed to obtain a semi-algebraic description of the admissible set:

$$S_D^p = \{D \in \mathbb{R}^6 \mid d_0 = 0 \mid g_w(D) \le 0, \quad \forall w \in \{\overline{x}, \underline{x}, \overline{y}, \underline{y}, \overline{z}, \underline{z}\}\}, \quad (13)$$

where the functions $g_w(D)$ are polynomials function in $d_1,\ d_2$ and d_3.

3. EVENT-BASED ALGORITHM

In this section, the control and trigger laws that constitute the event-triggered controller are designed. One must notice that the trigger law determines when to apply a suitable control law.

3.1 Control law

Tschauner (1967) demonstrated that the in-plane and out-of-plane control motions are decoupled and thus control problem can be treated separately.

In-plane control The in-plane motion is defined by the state subset $D_{xz}=[d_0, d_1, d_2, d_3]^T$. As stated earlier, periodicity is a desirable property to hover over a specified region, therefore, the in-plane control strategy aims to steer the system to a periodic orbit with one impulsive control. The in-plane state after an in-plane impulse $\Delta V_{xz}=[\Delta V_x, \Delta V_z]^T$ is given by $D_{xz}^+(\nu) = D_{xz}(\nu) + B_{D,xz}(\nu)\Delta V_{xz}(\nu)$ where $B_{D,xz}\in\mathbb{R}^{4\times 2}$ is composed of the in-plane terms of B_D. To obtain a periodic orbit, the state d_0 is steered to zero

$$d_0^+(\nu) = d_0(\nu) + B_{d_0,xz}(\nu)\Delta V_{xz}(\nu) = 0, \quad (14)$$

where $B_{d_i,xz}$ with i=0...3 is the (i+1)th row of $B_{D,xz}$. An impulse satisfying (14) can be written in general as

$$\Delta V_{xz}(\nu) = \lambda_{xz} B_{d_0,xz}^{\perp}(\nu) + \Delta V_{xz}^0(\nu), \quad (15)$$

where $\lambda_{xz}\in\mathbb{R}$, $B_{d_0,xz}^{\perp}\in\mathbb{R}^2$ describes the kernel space of $B_{d_0,xz}$ and $\Delta V_{xz}^0\in\mathbb{R}^2$ is any particular solution of (14). With this periodicity-pursuing strategy, the effect of an impulse on the current state D is described by

$$\begin{aligned} D_{xz}^+(\nu, \lambda_{xz}) =& D_{xz}(\nu) + \\ & B_{D,xz}(\nu)(\lambda_{xz} B_{d_0,xz}^{\perp}(\nu) + \Delta V_{xz}^0(\nu)). \end{aligned} \quad (16)$$

To maintain the state D_{xz} in the admissible set $S_{D_{xz}}^p$ at time ν, the following program is solved

$$\min_{\lambda_{xz}} \|\Delta V_{xz}(\nu, \lambda_{xz})\|_1, \quad \text{s.t.} \begin{cases} D_{xz}^+(\nu) \in S_{D_{xz}}^p, \\ \lambda_{xz} \in I_{sat,xz}(\nu), \end{cases} \quad \text{(Psat,in)}$$

where $I_{sat,xz}$ describes the input saturation and deadzone condition as a function of λ_{xz} and ν such that

$$\begin{aligned} I_{sat,xz} = \{\lambda_{xz} \in \mathbb{R} \text{ s.t. } & \\ \underline{\Delta V} \le |\lambda_{xz} B_{d_{0,xz}}^{\perp}(\nu) + \Delta V_{xz}^0(\nu)| \le \overline{\Delta V}\} = & \\ [\overline{l^-},\ \underline{l^-}] \cup [\underline{l^+},\ \overline{l^+}], & \end{aligned} \quad (17)$$

where $\overline{l^-}=(B_{d_{0,xz}^{\perp}})^+(-\overline{\Delta V} - \Delta V_{xz}^0)$, $\underline{l^-}=(B_{d_{0,xz}^{\perp}})^+(-\underline{\Delta V} - \Delta V_{xz}^0)$, $\overline{l^+}=(B_{d_{0,xz}^{\perp}})^+(\overline{\Delta V} - \Delta V_{xz}^0)$ and $\underline{l^+}=(B_{d_{0,xz}^{\perp}})^+(\underline{\Delta V} - \Delta V_{xz}^0)$.

Out-of-plane control The out-of-plane motion, represented by $D_y = [d_4, d_5]^T$, is naturally periodic and any out-of-plane impulse $\Delta V_y=\lambda_y$ produces a periodic orbit

$$D_y^+(\nu, \lambda_y) = D_y(\nu) + \lambda_y B_{D,y}(\nu), \quad (18)$$

where $B_{D,y}\in\mathbb{R}^2$ is composed of the out-of-plane terms of B_D. Consequently, to steer the state D_y to the admissible set $S_{D_y}^p$ at time ν, the following program is solved

$$\min_{\lambda_y} \|\Delta V_y(\nu, \lambda_y)\|_1, \quad \text{s.t.} \begin{cases} D_y^+(\nu) \in S_{D_y}^p, \\ \lambda_y \in I_{sat,y}, \end{cases} \quad \text{(Psat,out)}$$

where $I_{sat,y}$ describes the input saturation and deadzone conditions such that

$$I_{sat,y} = [-\overline{\Delta V},\ -\underline{\Delta V}] \cup [\underline{\Delta V},\ \overline{\Delta V}]. \quad (19)$$

Note that $I_{sat,y}$ does not depend on ν.

3.2 Instantaneous reachability conditions

To design the trigger rules, instantaneous S_D^p reachability conditions needs to be set at a given time instant ν. Note that, for the sake of clarity, the time dependence is omitted in this section. First, let the set Δ^+ be the reachable set from a given state D with one control. Δ^+ is a two-dimensional plane on the D space, defined by the lines Δ_{xz}^+ and Δ_y^+

$$\Delta_{xz}^+ = \{D_{xz}^+ \in \mathbb{R}^4 \text{ s.t. } (16), \lambda_{xz} \in \mathbb{R}\}, \quad (20)$$

$$\Delta_y^+ = \{D_y^+ \in \mathbb{R}^2 \text{ s.t. } (18), \lambda_y \in \mathbb{R}\}. \quad (21)$$

A necessary condition for the admissible set S_D^p to be reachable is that the following sets Λ_{xz}^+ and Λ_y^+ are non-empty:

$$\Lambda_{xz}^+ = [\underline{l_{xz}}, \overline{l_{xz}}], \quad (22)$$

$$\Lambda_y^+ = [\underline{l_y}, \overline{l_y}]. \quad (23)$$

The intervals $[\underline{l_{xz}}, \overline{l_{xz}}]$ and $[\underline{l_y}, \overline{l_y}]$ are computed such that at a given fixed instant ν

$$\begin{aligned} \forall \lambda_{xz} \in [\underline{l_{xz}}, \overline{l_{xz}}] : \{ & g_{\overline{x}}(\lambda_{xz}) \le 0,\ g_{\underline{x}}(\lambda_{xz}) \le 0, \\ & g_{\overline{z}}(\lambda_{xz}) \le 0,\ g_{\underline{z}}(\lambda_{xz}) \le 0\}, \end{aligned} \quad (24)$$

$$\forall \lambda_y \in [\underline{l_y}, \overline{l_y}] : \{g_{\overline{y}}(\lambda_y) \le 0,\ g_{\underline{y}}(\lambda_y) \le 0\}. \quad (25)$$

Note that the univariate polynomials $g_w(\cdot)$ are obtained by introducing (16) and (18) respectively in polynomial expressions $g_{\overline{x}}(d_1, d_2, d_3)$ and $g_{\underline{x}}(d_1, d_2, d_3)$, $g_{\overline{z}}(d_1, d_2)$ and $g_{\underline{z}}(d_1, d_2)$, $g_{\overline{y}}(d_4, d_5)$ and $g_{\underline{y}}(d_4, d_5)$ from Arantes Gilz et al. (2017). Moreover, accounting for the saturation and deadzone conditions (10), S_D^p is reachable if and only if the sets $\Lambda_{sat,xz}^+$ and $\Lambda_{sat,y}^+$ are non-empty:

$$\Lambda_{sat,xz}^+ = [\underline{l_{xz}}, \overline{l_{xz}}] \cap I_{sat,xz} \neq \emptyset, \quad (26)$$

$$\Lambda_{sat,y}^+ = [\underline{l_y}, \overline{l_y}] \cap I_{sat,y} \neq \emptyset. \quad (27)$$

Note that the sets of reachable admissible states, $\Delta^+_{sat,xz}$ and $\Delta^+_{sat,y}$, are given by

$$\Delta^+_{sat,xz} = \{D^+_{xz} \in \mathbb{R}^4 \text{ s.t. } (16), \lambda_{xz} \in \Lambda^+_{sat,xz}\}, \quad (28)$$

$$\Delta^+_{sat,y} = \{D^+_{y} \in \mathbb{R}^2 \text{ s.t. } (18), \lambda_{y} \in \Lambda^+_{sat,y}\}. \quad (29)$$

Let us define the following variables that measure the length of the intervals $\Lambda^+_{sat,xz}$ and $\Lambda^+_{sat,y}$ and its time derivative

$$L_{xz} = \text{len}(\Lambda^+_{sat,xz}), \quad L_y = \text{len}(\Lambda^+_{sat,y}), \quad (30)$$

$$L_{\nu,xz} = \frac{dL_{xz}}{d\nu}, \quad L_{\nu,y} = \frac{dL_y}{d\nu}. \quad (31)$$

These variables will be used as indicators for the S^p_D instantaneous reachability in the trigger rules of Section 3.4.

3.3 Reachability conditions over one period

In the previous section, instantaneous reachability conditions on S^p_D are found for a given instant ν. This section establishes that S^p_D is reachable over the next 2π-period (a complete revolution) if $D \in \mathcal{D}_c$ being $\mathcal{D}_c$ the invariant set of current D states, assuming that D is an equilibrium point ($d_0 = 0$), from which S^p_D can be reached in less than one period by applying a constrained impulse. Recalling that the control matrix B_D is 2π-periodic, computing the reachable set from a given state over a 2π-period can be done through implicitization techniques. In order to simplify the notation, the state increment is introduced as

$$\begin{aligned}\Delta D(\nu) &= D^+(\nu) - D(\nu) = B_D(\nu)\Delta V(\nu) \\ &= [\Delta d_0,\ \Delta d_1,\ \Delta d_2,\ \Delta d_3,\ \Delta d_4,\ \Delta d_5]^T. \end{aligned} \quad (32)$$

Considering the out-of-plane motion, the state increment is represented by $\Delta D_y = [\Delta d_4(\nu),\ \Delta d_5(\nu)]$. The incremental reachable set over an orbital period depends on the control effort λ_y and is implicitly described by

$$f_y(\Delta D, \lambda_y) = \frac{\Delta d_4^2}{\left(\frac{\lambda_y}{k^2\sqrt{1-e^2}}\right)^2} + \frac{\left(\Delta d_5 + \frac{e\lambda_y}{k^2(1-e^2)}\right)^2}{\left(\frac{\lambda_y}{k^2(1-e^2)}\right)^2} - 1 = 0. \quad (33)$$

Note that (33) is an ellipse in the Δd_4-Δd_5 plane. Its semi-axes and center are both affected by the control parameter, λ_y. Hence, for given deadzone and saturation conditions $\lambda_y \in I_{sat}$, the out-of-plane incremental reachable set is described by

$$\mathcal{D}_{f_y} = \mathcal{D}_{f_y,-} \cup \mathcal{D}_{f_y,+}, \quad (34)$$

where

$$\begin{aligned}\mathcal{D}_{f_y,-} := \{\Delta D \in \mathbb{R}^6 : & f_y(\Delta D, -\underline{\Delta V}) \geq 0, \\ & f_y(\Delta D, -\overline{\Delta V}) \leq 0\}. \end{aligned} \quad (35)$$

$$\begin{aligned}\mathcal{D}_{f_y,+} := \{\Delta D \in \mathbb{R}^6 : & f_y(\Delta D, \underline{\Delta V}) \geq 0, \\ & f_y(\Delta D, \overline{\Delta V}) \leq 0\}. \end{aligned} \quad (36)$$

Finally, the out-of-plane invariant set $\mathcal{D}_{c,out}$ is obtained computing the Minkowski sum of $S^p_{D_y}$, the admissible set, with the out-of-plane incremental reachable set (34),

$$\mathcal{D}_{c,\text{out}} := S^p_{D_y} \oplus \mathcal{D}_{f_y}. \quad (37)$$

Regarding the in-plane motion, both in-track (x) and radial (z) constraints have to be addressed. The in-plane control action, (16), can be implicitized for $d_0 \approx 0$ using a Gröbner basis as in Fix et al. (1996)

$$4\Delta d_1^2 + (-e^2+4)\Delta d_2^2 + 2e\Delta d_2\Delta d_3 - \Delta d_3^2 = 0. \quad (38)$$

Note that (38) is the equation of a cone representing the unconstrained in-plane incremental reachable set over a target orbital period. The control constraints (17) can be considered numerically by computing the instantaneous reachability at discrete times over one period for a large number of discrete points. The set of points with any $L_{xz}(\nu_p) \neq 0$ for $\nu_p \in [\nu, \nu + 2\pi]$ define $\mathcal{D}_{c,in}$.

In conclusion, S^p_D is reachable over a 2π-period if and only if $D \in \mathcal{D}_c = \mathcal{D}_{c,\text{in}} \times \mathcal{D}_{c,\text{out}}$.

3.4 Trigger law

The trigger law is designed to achieve a threefold objective. Firstly the programs (Psat,in) and (Psat,out) have to be feasible when executed. Secondly, unnecessary controls must be avoided. Finally, Zeno phenomena should be precluded.

This trigger law is defined by Algorithm 1 which induces the computation and execution of a control impulse based on given conditions. Each time the spacecraft leaves the admissible set S^p_D based on (13), the trigger variables L_{xz} and L_y are checked. If they are diminishing and below a threshold δ an impulse is commanded, whereas if they are null ($S^p_D \cap \Delta^+_{sat} = \emptyset$) the reachability over one period, $\mathcal{D}_c$, is computed to check the existence of future comeback opportunities. In the disfavourable case that these opportunities vanish the global stabilizing controller of Arantes Gilz et al. (2019), which ensures the return of the vehicle to S^p_D by applying three impulses, is commanded.

Algorithm 1 (Trigger rules)

Input: ν, D
Output: control decision
if $D \in S^p_D$ **then**
  Wait.
else if $D \notin S^p_D$ **and** $D \in \mathcal{D}_c$ **then**
  if $L_{xz}(\nu) < \delta$ **and** $L_{\nu,xz}(\nu) < 0$ **and** $L_y(\nu) < \delta$ **and** $L_{\nu,y}(\nu) < 0$ **then**
    Solve (Psat,in) and (Psat,out), apply ΔV_{xz} and ΔV_y.
  else if $L_{xz}(\nu) < \delta$ **and** $L_{\nu,xz}(\nu) < 0$ **then**
    Solve (Psat,in) and apply ΔV_{xz}.
  else if $L_y(\nu) < \delta$ **and** $L_{\nu,y}(\nu) < 0$ **then**
    Solve (Psat,out) and apply ΔV_y.
  else
    Wait
  end if
else if $D \notin \mathcal{D}_c$ **then**
  Apply the controller of Arantes Gilz et al. (2019)
end if

4. INVARIANCE OF THE SINGLE-IMPULSE APPROACH

In this section, the invariance of the proposed event-based predictive controller is studied. Firstly, some fundamental results of invariance for hybrid impulsive systems are summarized. Then the out-of-plane and in-plane invariance are analyzed.

The relative motion between target and chaser is equivalent to an hybrid impulsive system composed of the continuous dynamics of (1) and the resets of (8). Therefore, the

main results of Haddad et al. (2006) regarding invariance principles for hybrid impulsive systems apply. Consider the following dynamical system $\mathcal{G}$

$$\begin{array}{ll} \dot{x}(t) &= f_c(x(t)),\ x(0)=x_0,\ x_0\in\mathcal{D},\quad x(t)\notin\mathcal{Z},\\ \Delta x(t) &= f_d(x(t)), \qquad\qquad\qquad\quad x(t)\in\mathcal{Z}, \end{array} \quad (\mathcal{G})$$

where Δx denotes the instantaneous change on the state x due to an impulse f_d. Now, consider the following assumption over the hybrid system $\mathcal{G}$.

Assumption 1 (Haddad et al. (2006)): assume $f_c(\cdot)$ is locally Lipschitz continuous on $\mathcal{D}$, $\mathcal{Z}$ is closed, and $f_d(x)\neq 0$ for $x\in\mathcal{Z}\backslash\partial\mathcal{Z}$. If $x\in\partial\mathcal{Z}$ is such that $f_d(x)=0$, then $f_c(x)=0$. If $x\in\mathcal{Z}$ is such that $f_d(x)\neq 0$, then $x+f_d(x)\notin\mathcal{Z}$.

If Assumption 1 holds, then the following theorem applies.

Theorem 1 (Haddad et al. (2006)): consider the system $\mathcal{G}$, assume $\mathcal{D}_c\subset\mathcal{D}$ is a compact positively invariant set with respect to $\mathcal{G}$, and assume that there exist a continuously differentiable function $V:\mathcal{D}_c\to\mathbb{R}$ such that

$$V'(x)f_c(x)\leq 0, \qquad x\in\mathcal{D}_c,\ x\notin\mathcal{Z}, \quad (39)$$

$$V(x+f_d(x))\leq V(x), \qquad x\in\mathcal{D}_c,\ x\in\mathcal{Z}. \quad (40)$$

Let $\mathcal{R}\triangleq\{x\in\mathcal{D}_c : x\notin\mathcal{Z}, V'(x)f_c(x)=0\}\cup\{x\in\mathcal{D}_c : x\in\mathcal{Z}, V(x+f_d(x))=V(x)\}$ and let $\mathcal{M}$ denote the largest invariant set contained in $\mathcal{R}$. If $x_0\in\mathcal{D}_c$, then $x(t)\to\mathcal{M}$ as $t\to\infty$.

Considering Assumption 1 and Theorem 1, let us prove this proposition.

Proposition 1: under the trigger law of Algorithm 1, consider $x\in\mathcal{M}$ with $\mathcal{M}$ an invariant set such that $\mathcal{M}\subset\mathcal{D}_c$ and $\partial\mathcal{M}\cap\partial\mathcal{D}_c=\emptyset$. Then, if $y_0=x+\delta x\notin\mathcal{M}$, $y(t)\to\mathcal{M}$ as $t\to\infty$.

Proof: if both Assumption 1 and Theorem 1 are verified, as soon as $x+\delta x$ is outside $\mathcal{M}$ it can be guaranteed that the trigger law activates and will always command, through Algorithm 1, a single impulse steering back the state to the admissible set, $y\in S_D^p$, $S_D^p\subset\mathcal{M}$ if and only if $\mathcal{M}\subset\mathcal{D}_c$ and $\partial\mathcal{M}\cap\partial\mathcal{D}_c=\emptyset$.

Note that Proposition 1 implies a sufficient condition for the invariance of the set S_D^p in the presence of continuous disturbances. In the sequel, Proposition 1 conditions are checked for the proposed event-triggered controller.

Assumption 1 hypothesis are easily verified since (1) is Lipschitz continuous for $e\in[0,1)$ and the trigger signal is based on a closed domain S_D^p. Demonstrating the fulfillment of Theorem 1 needs more elaboration by proposing suitable V functions for each constraint defining S_D^p.

Regarding the invariance of the out-of-plane admissible set $S_{D_y}^p$, the following continuously differentiable function is proposed

$$V_{y_m}=g_{y_m}=(d_4-ey_m)^2+d_5^2-y_m^2, \quad (41)$$

which is the same expression of the out-of-plane constraint described by $g_{\underline{y}}$ and $g_{\overline{y}}$. Note that for both $\underline{y}$ and $\overline{y}$ constraints, Theorem 1 is fulfilled as

$$\frac{\partial V_{y_m}(D)}{\partial D}D'(\nu)=0, \qquad D\in\mathcal{D}_{c,\text{out}},\ D\in S_{D_y}^p, \quad (42)$$

$$V_{y_m}(D^+)\leq V_{y_m}(D), \quad D\in\mathcal{D}_{c,\text{out}},\ D\notin S_{D_y}^p, \quad (43)$$

where $\mathcal{D}_{c,\text{out}}$ has been obtained in (37). On the other hand, $\mathcal{M}_{\text{out}}=S_{D_y}^p\cup\underline{\mathcal{D}}_{c,\text{out}}$ is the union of the out-of-plane admissible set and the deadzone set $\underline{\mathcal{D}}_{c,\text{out}}:=\{D\in\mathcal{D}_{c,\text{out}},\ \text{s.t. } V_{y_m}(D^+)=V_{y_m}(D), D\notin S_{D_y}^p\}$. Finally, note that Proposition 1 holds since $\mathcal{M}_{\text{out}}\subset\mathcal{D}_{c,\text{out}}$ and $\partial\mathcal{M}_{\text{out}}\cap\partial\mathcal{D}_{c,\text{out}}=\emptyset$ as it can be deduced from (37) which is the Minkowski sum of a convex bounded set with an ellipse having a hole on its interior.

a = 8750 km, e=0.2, ν_0=0,
$\underline{\Delta V}$=1·10^{-3} m/s, $\overline{\Delta V}$=0.1 m/s
Initial relative position: [400, 300, -40] m
Initial relative velocity: [0, 0, 0] m/s
[$\underline{x}$, $\overline{x}$, $\underline{y}$, $\overline{y}$, $\underline{z}$, $\overline{z}$]=[50, 150, -25, 25, -25, 25] m

Table 1. Scenario parameters

For the in-plane case, the invariance is demonstrated, *mutatis mutandi*, in the same manner by using the following candidate functions for Theorem 1, $V_{x_m}=\hat{g}_{x_m}=\sum_{i=0}^{4}\overline{\theta}_{x_m,i}(d_1,d_2)d_3^i$, $V_{z_m}=g_{z_m}=d_1^2+d_2^2-z_m^2$. The necessary and sufficient conditions $\mathcal{M}_{\text{in}}\subset\mathcal{D}_{c,\text{in}}$ and $\partial\mathcal{M}_{\text{in}}\cap\partial\mathcal{D}_{c,\text{in}}=\emptyset$ are verified with the numerically obtained set $D_{c,\text{in}}$ so that Proposition 1 holds for given values of deadzone $\underline{\Delta V}$ and saturation $\overline{\Delta V}$.

5. SIMULATION RESULTS

To assess the performance of the proposed event-triggered predictive controller, a hovering phase scenario described in Table 1 is run. The simulation is done in MATLAB/Simulink using a non-linear relative motion simulator from Arantes Gilz (2016). Note that non-Keplerian forces such as the $J2$ effect and atmospheric drag are introduced as disturbances to both chaser and target vehicle.

Since the initial state is far from the admissible set, the 3-impulsive controller from Arantes Gilz et al. (2019) is used to reach S_D^p. Then, the local event-based controller takes the lead as soon as S_D^p is reached. The controller threshold is δ=0.07 and the sampling rate is such that the trigger rules of Algorithm 1 are evaluated every 5° (in terms of true anomaly) along 10 target orbital periods. As seen in

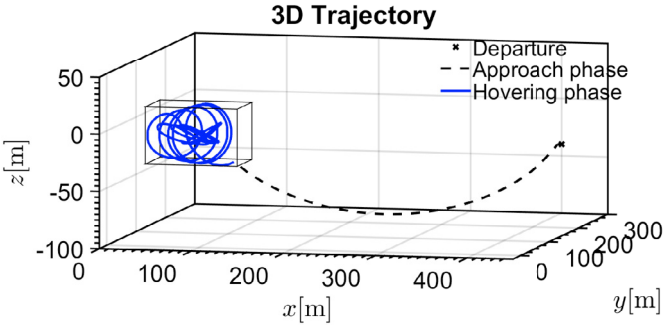

Fig. 1. Spacecraft trajectory.

Fig.1, the event-triggered predictive controller achieves its purpose of maintaining the spacecraft close to the hovering zone. The commanded impulses, the trigger variables, L_{xz} and L_y, and the commanded control are shown in Fig.2. The limitation imposed by the deadzone condition can be observed in the out-of-plane control as well as the more consuming in-plane control. Table 2 compares the local controller of this work with the global controller from Arantes Gilz et al. (2019). The comparison begins when the hovering zone is reached and is carried out over 10 orbits. The considered parameters for the global controller

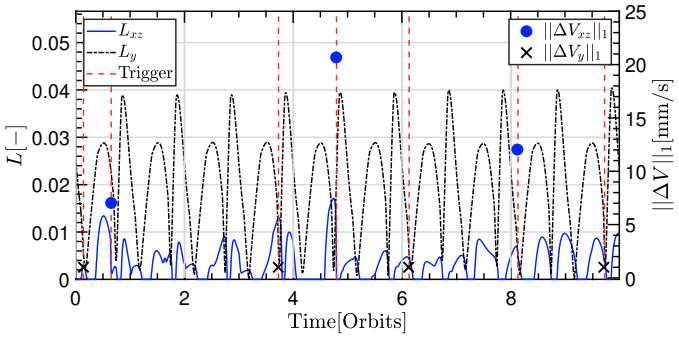

Fig. 2. Plot of L_{xz}, L_y, trigger signal, $\|\Delta V_{xz}\|_1$ and $\|\Delta V_y\|_1$.

	J[cm/s]	N[-]	$X \in$ box[%]
Local	4.375	7	98.26
Global	6.336	15	94.44

Table 2. Comparison between local and global controllers.

are τ_I=τ_E=5° and τ_S=60°. For the considered scenario, the event-triggered controller improves the performance criteria in terms of fuel consumption, J=$\sum_{i=1}^{N}\|\Delta V_i\|_1$, number of impulses N and the amount of time X is in the hovering box. The fuel consumption only accounts for applied impulses control. For instance, when the global controller computes impulses that fall within the deadzone, they are set to zero and are not considered in the cost J. The criterion "$X \in$ box" indicates the percentage of time that the chaser spacecraft lays inside the hovering box which is the primary goal of the hovering phase.

6. CONCLUSIONS

In this paper, an event-triggered predictive controller is employed to locally maintain the spacecraft within the limits of the hovering zone, under both deadzone and saturation in the actuation. An invariance analysis for the proposed approach has been done by using impulsive hybrid systems theory combined with reachability techniques. The outcome of the invariance study is that the proposed controller guarantees the return of the spacecraft to the hovering zone under the presence of continuous perturbations that may expel the vehicle out of the admissible set. A numerical simulation has been carried out for a typical hovering scenario which shows the potential benefits of the event-triggered approach when compared with a periodic controller. The main drawback of the proposed algorithm is that the robustness of the method under impulse misexecution has not been addressed yet. Future work may include a more formal analysis of the in-plane invariance and the robustification of the controller under impulses mishaps.

REFERENCES

Arantes Gilz, P.R. (2016). A Matlab®/Simulink® non-linear simulator for orbital spacecraft rendezvous applications. URL `https://hal.archives-ouvertes.fr/hal-01413328`.

Arantes Gilz, P.R., Joldes, M., Louembet, C., and Camps, F. (2017). Model predictive control for rendezvous hovering phases based on a novel description of constrained trajectories. In *IFAC World Congress*, pp. 7490–7495. Toulouse, France.

Arantes Gilz, P.R., Joldes, M., Louembet, C., and Camps, F. (2019). Stable model predictive strategy for rendezvous hovering phases allowing for control saturation. Accepted in *Journal of Guidance, Control and Dynamics*. URL `https://hal.archives-ouvertes.fr/hal-01678768`.

Aström, K.J. (2008). *Analysis and Design of Nonlinear Control Systems*, chapter Event Based Control, 127–147. Springer, Berlin, Heidelberg.

B. Reed, B., C. Smith, R., Naasz, B., F. Pellegrino, J., and E. Bacon, C. (2016). The Restore-L servicing mission. In *AIAA Space*.

Barnhart, D., Sullivan, B., Hunter, R., Bruhn, J., Fowler, E., M. Hoag, L., Chappie, S., Henshaw, G., E. Kelm, B., Kennedy, T., Mook, M., and Vincent, K. (2013). Phoenix Project status - 2013. In *AIAA Space*.

Breger, L.S. and How, J.P. (2008). Safe trajectories for autonomous rendezvous of spacecraft. *Journal of Guidance, Control and Dynamics*, 31(5), 1478–1489.

Brentari, M., Urbina, S., Arzelier, D., Louembet, C., and Zaccarian, L. (2018). A hybrid control framework for impulsive control of satellite rendezvous. *IEEE Transactions on Control Systems Technology*, 1–15.

Deaconu, G. (2012). Constrained periodic spacecraft relative motion using non-negative polynomials. *American Control Conference*, 6715–6720.

Deaconu, G. (2013). *On the trajectory design, guidance and control for spacecraft rendezvous and proximity operations*. Ph.D. thesis, Univ. Toulouse 3 - Paul Sabatier, Toulouse, France.

Di Cairano, S., Park, H., and Kolmanovsky, I. (2012). Model predictive control approach for guidance of spacecraft rendezvous and proximity maneuvering. *International Journal of Robust and Nonlinear Control*, 22(12), 1398–1427.

Fix, G., Hsu, C.P., and Luo, T. (1996). Implicitization of rational parametric surfaces. *Journal of Symbolic Computation*, 21(3), 329 – 336.

Gaias, G. and D'Amico, S. (2015). Impulsive maneuvers for formation reconfiguration using relative orbital elements. *Journal of Guidance, Control and Dynamics*, 38(6), 1036 – 1049.

Haddad, W.M., Chellaboina, V., and Nersesov, S.G. (2006). *Impulsive and Hybrid Dynamical Systems*, chapter Stability Theory for Nonlinear Impulsive Dynamical Systems, 9–80. Princeton Series in Applied Mathematics.

Louembet, C. and Arantes Gilz, P.R. (2018). Event-triggered model predictive control for spacecraft rendezvous. In *6th IFAC Conference on Nonlinear Model Predictive Control*. Madison, USA.

Pawlowski, A., Guzmán, J., Berenguel, M., and Dormido, S. (2015). *Event-Based Generalized Predictive Control*, 151–176.

Qi, R., Xu, S., and Xu, M. (2012). Impulsive control for formation flight about libration points. *Journal of Guidance, Control and Dynamics*, 35(2), 484–496.

Tschauner, J. (1967). Elliptic orbit rendezvous. *AIAA Journal*, 5(6), 1110–1113.

Wu, B., Shen, Q., and Cao, X. (2018). Event-triggered attitude control of spacecraft. *Advances in Space Research*, 61, 927–934.

Wu, W., Reimann, S., and Liu, S. (2014). Event-triggered control for linear systems subject to actuator saturation. In *19th IFAC World Congress*. Cape Town, South Africa.

Yamanaka, K. and Ankersen, F. (2002). New state transition matrix for relative motion on an arbitrary elliptical orbit. *Journal of Guidance, Control, and Dynamics*, 25(1), 60–66.

Yang, X. and Cao, X. (2015). A new approach to autonomous rendezvous for spacecraft with limited impulsive thrust: Based on switching control strategy. *Aerospace Science and Technology*, 43, 454–462.

Zhang, C., Wang, J., Sun, R., Zhang, D., and Shao, X. (2018). Multi-spacecraft attitude cooperative control using model-based event-triggered methodology. *Advances in Space Research*, 62, 2620–2630.